PCCP

Cite this: *Phys. Chem. Chem. Phys.*, 2011, **13**, 3886–3895

www.rsc.org/pccp

PAPER

A periodic mixed gaussians–plane waves DFT study on simple thiols on Au(111): adsorbate species, surface reconstruction, and thiols functionalization†

Gopalan Rajaraman,‡ Andrea Caneschi, Dante Gatteschi and Federico Totti*

Received 5th October 2010, Accepted 30th November 2010
DOI: 10.1039/c0cp02042g

Here we present DFT calculations based on a periodic mixed gaussians/plane waves approach to study the energetics, structure, bonding of SAMs of simple thiols on Au(111). Several open issues such as structure, bonding and the nature of adsorbate are taken into account. We started with methyl thiols (MeSH) on Au(111) to establish the nature of the adsorbate. We have considered several structural models embracing the reconstructed surface scenario along with the $MeS^{\bullet}$–Au_{ad}–$MeS^{\bullet}$ type motif put forward in recent years. Our calculations suggest a clear preference for the homolytic cleavage of the S–H bond leading to a stable $MeS^{\bullet}$ on a gold surface. In agreement with the recent literature studies, the reconstructed models of the $MeS^{\bullet}$ species are found to be energetically preferred over unreconstructed models. Besides, our calculations reveal that the model with 1 : 2 Au_{ad}/thiols ratio, *i.e.* $MeS^{\bullet}$–Au_{ad}–$MeS^{\bullet}$, is energetically preferred compared to the clean and 1 : 1 ratio models, in agreement with the experimental and theoretical evidences. We have also performed Molecular Orbital/Natural Bond Orbital, MO/NBO, analysis to understand the electronic structure and bonding in different structural motifs and many useful insights have been gained. Finally, the studies have then been extended to alkyl thiols of the RSR′ (R, R′ = Me, Et and Ph) type and here our calculations again reveal a preference for the $RS^{\bullet}$ type species adsorption for clean as well as for reconstructed 1 : 2 Au_{ad}/thiols ratio models.

1. Introduction

Self-assembled monolayers (SAMs) of functionalized organic/inorganic moieties have a great potential for applications in nanoproduction, spintronics, biological sensoring, *etc.*[1–7] Single atoms or molecules once grafted onto a metal surface can keep their peculiar behavior as in the isolated phase and/or exhibit different and unprecedented properties from the bulk/isolated ones. Such properties can range from the coupling of the SAMs with the electronic and optical properties of a metallic surface to the linking of macroscopic interfacial phenomena to molecular-level structures.[3] Magnetic properties have long been neglected but recently several attempts have been made to assemble layers of Single Molecule Magnets (SMMs) with alkyl thiol groups in a bottom up approach to build magnetic memory banks.[8–15] Encouraging results in this direction have been reported where magnetic hysteresis was observed at low temperature.[15] Exciting as these systems can be, they are rather complex and a deep understanding of the substrate–magnetic molecule interaction is still very difficult. In order to gain deeper insight SAMs of simpler magnetic molecules, like nitronyl nitroxide radicals (NitR), on gold were reported.[16–19] Among several derivatives studied the 4-(methylthio)phenyl nitronyl nitroxide and 4-(methylthio)methyl phenyl nitronyl nitroxide form stable and ordered SAMs[16] which keep the radical nature on the gold surface. The use of a stable radical can provide information not only on the structural arrangement of the thiols on the metal surface but also on the dynamics of the organized molecules. However, to get a deep insight on the structural and magnetic properties of such complex systems by using DFT,[20] a reliable computational approach should be established. Therefore we decided to start a sort of benchmarking work for the naked thiols to check if our computational protocol based on a mixed Gaussian and plane waves approach (GPW) could be reliable enough compared to experimental and already published theoretical works. In fact, alkyl thiols $CH_3(CH_2)_n$–SH absorbed mostly on (111) faces of coinage metal surfaces are, probably, the most studied SAMs

Dipartimento di Chimica, Polo Scientifico, INSTM Università degli Studi di Firenze, via della Lastruccia 3, 50019 Sesto fiorentino, Italy. E-mail: federico.totti@unifi.it
† Electronic supplementary information (ESI) available: Structural and thermodynamic data. See DOI: 10.1039/c0cp02042g
‡ Present address: Department of chemistry, Indian Institute of Technology Bombay, Mumbai-400076, India.

both at the experimental and, even more, at the theoretical level.[1–7,21–52] Despite many efforts, the detailed nature in the "standing up" phase of the interface structures is still a subject of debate.[21–52] Early experimental reports on the nature of the alkyl thiol interaction with the gold surface showed a $(\sqrt{3} \times \sqrt{3})R30^\circ$ (from now on $\sqrt{3}$) structure for methyl thiols and a c(2 × 4) superstructure for longer chain alkane thiols. These data show that the bridge site, slightly displaced towards an fcc (face-centered cubic) site, is the preferred attacking site of the S head group on the Au(111) surface.[22–31] Recent experimental results showed that in thiol SAMs on Au(111) the S head group can adsorb on the top of gold adatoms which occupy threefold hollow sites.[32–34] However, very recent experimental and theoretical reports claim a complex behavior where one adatom (Au_{ad}) sandwiched between two thiol molecules (*i.e.* MeS–Au_{ad}–MeS type species) is energetically the most favourable.[6,35–52] The most recent works demonstrated the increased Au–S bond stability in the presence of defects of the Au(111) surface as adatoms and/or vacancies.[40] Based on the molecular dynamics and *ab initio* studies,[37,51] it has been suggested that the bridge conformation to $MeS^{\bullet}$–Au_{ad}–$MeS^{\bullet}$ conversion by pulling an Au atom from the surface is feasible. The c(2 × 4) superstructure has also been suggested to be more stable for long chain alkyl thiol SAMs.[39,44,45] On the other hand, all the theoretical works presented to-date do not give a general picture related to the absorption problem, since all of them were limited to the study of a single or two reacting species. Moreover, since most of the studies used DFT based approaches, the choice of different functionals and basis sets made it difficult to compare the data among different papers.[35–52] Despite such extensive studies over the years on the alkyl thiols, many fundamental issues are still poorly understood such as the mechanism of adsorption, nature of adsorbed species and site of adsorption and the nature of interaction between adsorbed species and the gold surface.

In this work we would like to give a more complete overview on the energetics and the nature of the many possible structural motifs on the clean and reconstructed Au(111) surface involved in the formation of the alkyl thiol using the periodic density functional theory with a mixed Gaussian and plane wave method implemented in a CP2K software package.[53–56] Our study includes most of the basic model structure proposed so far of alkyl thiol on Au(111) and additionally we have also tested few other models. Significant insights into the bonding of these structural motifs have been gained from the NBO and MO analyses.

2. Computational details

All calculations have been performed with DFT implemented in the CP2K program package[53–56] unless otherwise stated. The CP2K package adopts a hybrid basis set formalism known as a Gaussian and Plane Wave[56] (GPW) method where the Kohn–Sham orbitals are expanded in terms of contracted Gaussian type orbitals (GTO), while an auxiliary plane wave basis set is used to expand the electronic charge density. A double-ζ GTH basis set and its relativistic norm-conserving pseudo potentials (Goedecker, Teter, and Hutter)[56] were used in addition to a plane wave basis set with an energy cut-off of 350 Ry. The cut-off value has been estimated by performing a series of single point calculations on a 36 atoms gold cell comprising 12 gold atoms in each layer, with different cut-off values until no significant variation in the computed energy was observed.

BLYP[57,58] and TPSS[59] are the density functionals used throughout the calculations performed with the CP2K package.

The validity of the CP2K package as an accurate k-point only approach has been validated through a systematic super-cell approach for the calculation of transition metal surface properties.[60,61] Three different unit cells comprising 36, 48 and 54 gold atoms have been built and employed throughout the study. The unit cells were shaped to obtain in all cases three layers of the Au(111) surface when the period boundary conditions are imposed over an orthorhombic simulation cell. The adatom cases were studied by positioning one or two adatoms on the top of the layer and in all cases the adatom positions were relaxed without any constraints to their positions. In the case of imposed vacancies, the layer was kept frozen. The convergence criteria of 1×10^{-7} Hartree for the SCF energy and 9×10^{-4} Hartree $Å^{-1}$ (Hartree per Radians) for the energy gradient had been employed throughout.[61,62] The simulation cell has been defined with x and y axes on the surface plane as the reference axes. The cell size along the z axis was chosen to be 40 Å, compared to an inter-layer distance of 2.35 Å, to avoid unphysical interactions between repeated slabs. Unless otherwise stated in all calculations the gold layer has been kept frozen. The binding energies were computed according to the following expression[38]

$$\Delta E_{ads} = \frac{1}{n\mathrm{SR_1R_2}}[E(n\mathrm{R_1R_2S-Au(111)}) - E(\mathrm{Au(111)}) + - n\mathrm{SR_1R_2} \times E(\mathrm{SR_1R_2}) - n\mathrm{Au_{ad}} \times E(\mathrm{Au_{bulk}})]$$

where $n\mathrm{SR_1R_2}$ is the number of adsorbed alkane thiols, $E(\mathrm{R_1R_2S{-}Au(111)})$ is the energy of chemisorbed species on the Au(111), $E(\mathrm{Au(111)})$ is the energy of the clean Au(111) surface, $E(\mathrm{SR_1R_2})$ is the energy of unadsorbed alkane thiols, $E(\mathrm{Au_{bulk}})$ is the total energy of one gold atom in the bulk phase and the ΔE_{ads} being the binding energy for the adsorption process. By this definition, negative ΔE_{ads} values indicate an exothermic process. The three-layers thickness of the model has been justified by calculating the enthalpy of formation of an adatom and a vacancy for three, four and five layers on the 36 gold atoms cell. The choice of the model with three layers *vs.* five layers introduces *ca.* 5 kcal mol^{-1} error on adatom energy formation and 0.2 kcal mol^{-1} error on vacancy formation. Considering a large gain in the computational cost, the obtained differences are modest. Moreover the differences observed are expected to be nearly constant for the calculation of reaction energies for the current studied system. Therefore here we have chosen to study the system with three layer models.

NBO analysis has been computed using Jaguar[63] suits of packages with a hybrid B3LYP[64] functional together with a LACVP* basis set on the CP2K computed geometries.

The LACVP* basis set comprises the LanL2DZ*[65] basis set for gold and the 6-31G* basis set for other atoms.[66]

3. Results and discussion

Adsorption of methyl thiols on Au(111)

We begin with methyl thiols, the simplest of alkyl thiols where rich experimental and theoretical data are available.[1–7] The first issue we address here is the nature of adsorbate as this study will lay down foundation for studies on other alkyl thiols. There are conflicting experimental[3] and theoretical reports on the nature of the thiol adsorbate on Au(111). When thiols grow in a SAM it is unclear whether the H atom remains bonded to the S head group or forms thiolates (RS^-) or thiol radicals ($RS^\bullet$) by cleaving the S–H bond in a hetero- or homolytic fashion. The earlier experimental studies[67] and also some recent reports suggest the existence of intact thiols on the clean surface.[68] On the other hand there is a growing number of experimental[69] and theoretical evidence[70] suggesting that the thiolates are formed by cleaving the S–H bonds and leaving the sulfur head group to adsorb more firmly on the surface. No definitive evidence on the nature of the dissociative mechanism is however reported.

Three possible scenarios are taken into consideration when the surface structure is considered to be clean,

$$MeS\text{–}H + Au(111) \rightarrow MeSH\text{–}Au(111)\ [\text{non-dissociative}]$$

$$MeS\text{–}H + Au(111) \rightarrow MeS^\bullet\text{–}Au(111) + H^\bullet\ [\text{homolytic}]$$

$$MeS\text{–}H + Au(111) \rightarrow MeS^-\text{–}Au(111) + H^+\ [\text{heterolytic}]$$

The first one represents a non-dissociative mechanism where the S–H bond is intact during the adsorption; the second and third represent a dissociative mechanism where the S–H bond can cleave either homolytically or heterolytically, leaving a radical centre or a residual charge on the sulfur head group, respectively.

Unreconstructed surface

The computed binding energies of the three species are illustrated in Fig. S1 (ESI†)[19] and selected structural parameters are given in Table S1 (ESI†) along with a list of available experimental and theoretical results reported. For the two functionals tested, it is apparent that the TPSS always yields lower binding energy than the ones obtained with the BLYP. This is not surprising given the fact that although the BLYP functional can describe accurately the repulsive intermolecular forces that occur at short range, it fails in describing the attractive part of the van der Waals forces. This behavior is amended in the TPSS functional and this leads to reliable binding energy values as well as structural prediction[59] and its superiority in the performance over BLYP has been documented in a number of studies in the literature.[85–90] In the MeSH case, both functionals predict that the radical species is the energetically most favourable one with a binding energy of -37.2 kcal mol^{-1} with TPSS and -26.5 kcal mol^{-1} with the BLYP. The binding energy obtained with the TPSS is consistent with the reported experimental values (see Table S1, ESI†). For example, for the $MeS^\bullet$ species using a PBE functional a formation energy of -35.6 kcal mol^{-1} has been reported.[37] The non-dissociative MeSH adsorption is 24.4 kcal mol^{-1} higher in energy than that of the radical species while the charged S^- species is only 3.1 kcal mol^{-1} higher in energy. Additionally, in the homolytic-dissociative mechanism the formation of radical species is accompanied by the formation of H atom which upon recombination with another H atom can produce H_2 molecule. Another possible reaction is the one involving the absorption of the H atom directly on the gold surface. Here we consider only the former since it is the most likely process. In fact, the formation of H_2 at the surface during the adsorption process has been suggested in many instances[3,91,92] supporting the dissociative mechanism. A very recent experimental evidence based on X-ray photoelectron spectroscopy on the SAMs of some nitroaromatic thiols prepared by a vacuum vapour deposition technique, conclusively reveals the S–H cleavage and the reaction of the hydrogen with the one of the nitro groups.[93]

If we take into account the formation of H_2 molecule and thus the entire reaction, the formation energies should be computed with the following equation,

$$\Delta E_f = [E(Au_n\text{–}MeS^\bullet) + \tfrac{1}{2}E(H_2)] - [E(Au_n) + E(MeSH)]$$

This yields the formation energy as -7.2 kcal mol^{-1} for the radical reaction. The reaction is still an energetically favourable exothermic process. This result clearly demonstrates that on the clean surface the dissociative mechanism can occur during the adsorption process. The computed structures for the three species are different with respect to the functional employed—the BLYP predicts rather a physisorbed MeSH on the gold with the shortest S–Au bond length being 3.67 Å while the TPSS reveals a chemisorbed quasi-atop structure with an S–Au bond length of 2.61 Å. The computed structures differ among the three species: if MeSH adopts a quasi-atop structure, the MeS^- and $MeS^\bullet$ take on a bridge-fcc structure (TPSS functional), instead. The TPSS computed S–Au bond lengths for the MeS^- and $MeS^\bullet$ species are 2.59, 2.61 Å and 2.52, 2.55 Å, respectively, with the later having the shortest bond lengths (*i.e.* the strongest sulfur–gold interaction). The molecular tilt angle ζ is another important parameter which defines the orientation of the adsorbed species with respect to the surface normal and this can be estimated from the experimental data (see Table S1, ESI†), allowing a direct comparison to the computed structure possible. Among three structures the MeS^- has the lowest ζ (58.6°) while $MeS^\bullet$ and the MeSH have higher values: 56.6° and 69.1°, respectively. The tilt angle ζ can be seen as an index of the electron delocalisation of the adsorbate on the Au(111).[94]

The trend in ζ we observe is, therefore, in agreement with different charge accumulations observed for the three species. To understand the electronic structure in detail single point calculations and NBO analysis have been performed on the three different species with the TPSS Au_{36} atom cluster. Single point calculations have been performed using Jaguar at the B3LYP/LACVP* level without imposing periodic boundary conditions. The natural charges obtained *via* the NBO analysis of the adsorbed species together with the isolated species are

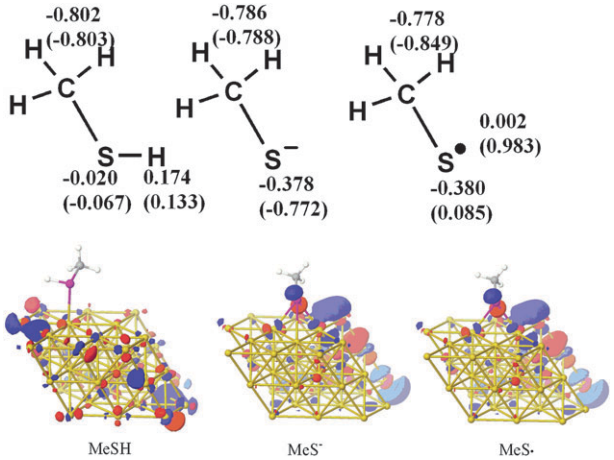

Fig. 1 The computed NBO charges, spin densities and HOMO plots of the three different species. The values given in the parentheses are for the isolated fragments. For the MeS• species along with the charges, the spin density on the sulfur has also been given for the MeS• and for the bare MeS• species (in parentheses).

given in Fig. 1. The NBO computed charges on the sulfur atom of the MeS^- and MeS• are similar for the adsorbed state. However, in the isolated scenario, only the MeS• species has a very small positive charge on the sulfur atom. This reveals the resemblance between the two species upon adsorption as there is a flow of electrons from the surface to the molecule for the MeS• species. This is also supported by the fact that the spin density on the sulfur atom diminishes from 0.983 to 0.002 during adsorption. The second order perturbative theory estimate of the donor–acceptor interactions in NBO can offer information on the Au–S bond stabilisation energies. The important stabilisation energies are listed in Table S1 (ESI†). The NBO analysis indicates a very strong σ-type $3p_z$(S)–6s(Au) interaction in MeSH species with a small σ-type 3s(S)–6s(Au) interaction (see Table S2, ESI†). The bonding scenarios for the MeS^- and MeS• are similar with a strong σ-type $3p_z$(S)–6s(Au) and weak 3s(S)–6s(Au), 3s(S)–$6p_z$(Au) interactions and a much weaker π-type $3p_x$(S)–6s(Au) interaction. According to the Newens–Anderson chemisorption model[95] the adsorbate's highest-occupied-molecular-orbital (HOMO) overlaps with the narrow d-band of the metal, producing hybrid bonding and antibonding orbitals. The HOMO plotted in Fig. 1 illustrates that both MeS^- and MeS• are in accord with this picture where the S–Au bond is described as an anti-bonding combination of the p-type MO of sulfur and the d-type MO of gold. The interaction with the two nearest gold atoms is antibonding.

However the sulfur p-type wave function tail has a bonding character mainly with the facing gold atom d-orbital, stabilizing the bridge configuration. It is worth to note here that, both MeS^- and MeS• have similar HOMO with a significant contribution from the sulfur atom. The density of states (DOS) (see Fig. S2, ESI†) is plotted for sulfur p-orbitals of the three species and the gold d-orbitals of the MeS• species. For sulfur the bonding and the anti-bonding peaks are close to each other, with the HOMO being the antibonding peak for all the three species. It is clear from MeS^- and MeS• DOS that both have very similar features while the MeSH DOS looks distinctly different—lacking the intense peak near the HOMO and having a most intense bonding peak at the lower end of the energy spectrum plotted. The gold d-orbitals are very similar in all three cases and thus they have not been shown for clarity. The DOS plots basically support the conclusions derived from the NBO results.

Reconstructed surface

The recent trend on the studies on alkyl thiols on Au(111) suggests that the Au(111) surface undergoes severe reconstruction during the adsorption process.[33–52] This eventually leads to the presence of Au adatoms and/or vacancies on the top layer of the Au(111). This demands revisions to the previously considered models as the presence of one or two Au_{ad} atoms/vacancies can remarkably change the structure as well as energetics of the SAM formation. In this regard several model structures have been put forth so far by experiments and theory.[33–52] The experimental studies using NIXSW analysis suggest that the sulfur head group occupies the atop site for the Au_{ad} atoms on the Au(111).[33] On the other hand low temperature STM studies as well as GIXRD analysis suggest the formation of the MeS–Au_{ad}–SMe type structure.[35,40,41,52] Apart from the convincing evidences

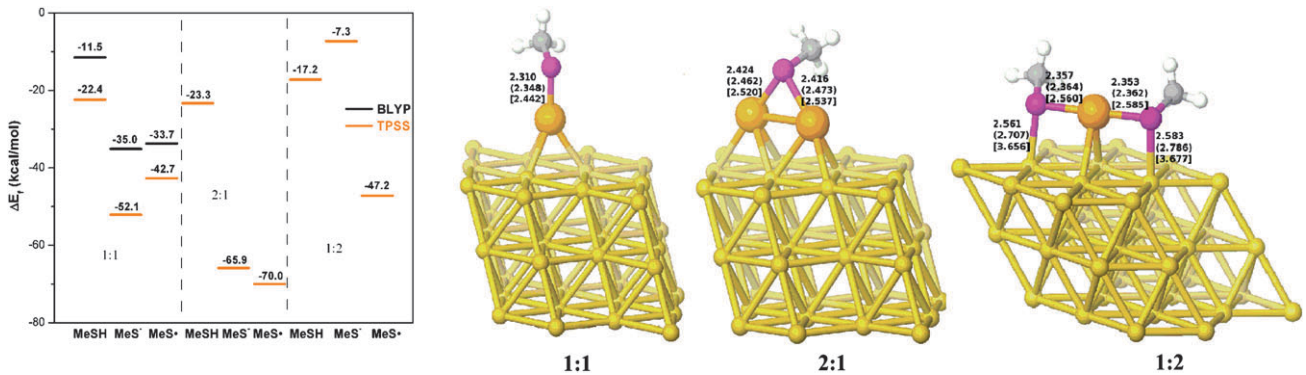

Fig. 2 The DFT computed binding energies of the three different species on the reconstructed Au(111) with one or two Au adatoms. The BLYP results have been presented only for the first species. The optimized structures shown are of the MeS• species computed using the TPSS functional. The bond lengths given in the parentheses are of MeS– (curved) and MeSH species [squared].

accumulated for the presence of Au_{ad} atoms, there are some experimental studies supported also by DFT calculations[39,40] which assume the presence of irregular vacancies on the top layer of Au(111). At the same time some reports suggest the presence of defects (vacancies) on the top layer of the Au(111) occurring together with the Au_{ad} formation.[40] A recent report on the mechanism of the formation suggests a facile low energy path for the conversion among different types of Au_{ad}/vacancies species.[51]

The energetics of the three species with several possible structural models are summarized in Fig. 2. The first model is based on the 1 : 1 ratio of Au_{ad}/MeSX (X = H, −, •), where the Au_{ad} and the MeSX are allowed to relax while the underlying surface structure is kept frozen. The calculations with BLYP and TPSS functionals on this model reveal that, as in the other cases, the TPSS yields lower formation energies than that of the BLYP functional and the TPSS computed structural parameters are in good agreement with the experimental data and other computational studies.[38,39,45] Based on those results, we have restricted our further studies only to the TPSS functional. There are two possibilities to place the Au_{ad} on the Au(111) surface: one is on the FCC hole and the other on the HCP hole. In all the three cases HCP is found to be more stable by 0.4, 2.9 and 1.1 kcal mol^{-1} with respect to the FCC site for the MeSH, MeS^- and $MeS^•$ species respectively. The energies given in Fig. 2 are related to the HCP site. Hereafter, we will focus on the HCP low energy structures for comparison. All the three species MeSH, MeS^- and $MeS^•$ adopt atop configuration on the Au_{ad} atom (a quasi-atop in the case of FCC site structures) with the formation energies of −22.4, −52.1 and −42.7 kcal mol^{-1} respectively. The computed energy of −42.7 for the $MeS^•$ species is comparable to −47.3 kcal mol^{-1} reported using the PBE functional.[37] It is important to note here that in the presence of Au_{ad} the MeS^- species is found to be more favourable than the $MeS^•$ one by 9.4 kcal mol^{-1}. This implies that in the presence of Au_{ad} the S–H cleavage should preferentially occur in a heterolytic fashion, in agreement with the observed pH dependency on the SAM formation.[96–98] The Au–S bonds are very short in these models and in fact the bond lengths fall in the range of Au–S bond lengths reported for molecular structures containing gold–sulfur bonds.[99] This suggests that there is a full Au–S bond here rather than chemisorbed weak interactions like those observed in the unreconstructed surfaces. The computed tilt angles ζ for the three species, MeSH, MeS^- and $MeS^•$, are 107.1°, 103.3° and 105.0° respectively. The trend is similar to the one found for the clean surface: the bond angles are slightly larger due to the absence of weak interactions between hydrogen atoms and the gold surface. The NBO analysis indicates a very strong σ-bond ($3p_z$(S)–6s(Au)) with a significant donation from the sulfur atom (more than 65%) in all the three species. The other σ-type 3S(S)–6s(Au) interaction is much weaker (see Table S2, ESI†) and due to atop configuration the π-type interactions are negligible. The perturbation analysis reveals that the Au–S bond in the MeSH species is *ca.* three times weaker than in MeS^- and $MeS^•$ species (see Table S2, ESI†). The computed structures and formation energies of the $MeS^•$ species are in good agreement with previously reported results.[45]

We also performed calculations on the $MeS^•$ species on a clean surface with a vacancy on the first layer. The optimised structure has the sulfur group sitting on the hexagonal vacancy hole with two short (2.91 and 2.90 Å) and four long Au–S bond lengths (in the range of ∼3.2–3.4 Å). The computed binding energy for this structure is −15.2 kcal mol^{-1} compared to −37.2 kcal mol^{-1} for the clean surface, supporting the findings that the formation of vacancies is not the energetically preferred model.[33,50] Therefore we have only considered the presence of Au_{ad} here after. A similar conclusion has also been obtained from theoretical studies on the ethyl thiol adsorption in Au(111).[51,54]

The second model is based on the 2 : 1 ratio of Au_{ad}/MeSX (*vide supra*), where two Au_{ad} are bonded together with one substrate being allowed to chemisorb. The computed binding energies resemble the trend found on the unreconstructed surface with the $MeS^•$ species being the most favourable with 4.1 and 46.9 kcal mol^{-1} margin for the MeS^- and MeSH species respectively. As in the other models non-dissociative MeSH species is highly unfavourable. All the three species adopt a bridge structure between the two Au_{ad} atoms with average Au_{ad}–S bond lengths of 2.53, 2.47 and 2.42 Å for the MeSH, MeS^- and $MeS^•$ species. The bonding scenarios between the non-dissociative MeSH and the dissociative MeS^- and $MeS^•$ species are very different. Since the MeSH species is in the bridging mode, unlike the atop model with one adatom, the predominant σ-type $3p_z$(S)–6s(Au) is absent and the dominant σ-type interaction here is 3s(S)–6s(Au) with a weaker π-type $3p_x$(S)–6s(Au) interaction (see Table S2, ESI†). This complies with lower binding energy compared to that of the single adatom case (29.7 *vs.* 46.7 kcal mol^{-1} gap from the respective favored species).

The dissociative MeS^- and $MeS^•$ species have a similar bonding frame, with a predominant σ-type $3p_z$(S)–6s(Au) interaction and a strong π-type $3p_x$(S)–6s(Au) interaction and the σ-type 3s(S)–6s(Au) interaction is less prominent than in MeSH.

The third model is based on the 1 : 2 ratio of Au_{ad}/methyl thiol, where the two adsorbates and an Au_{ad} are allowed to relax on the Au(111) surface. There are several experimental studies which support this ratio[43,52] while others contradict.[51] In particular, the study which focused on the structure of Au(111) after removing the adsorbate by reaction with hydrogen atoms claims that the Au_{ad} are indeed present on the surface in the 1 : 2 ratio of Au_{ad}/alkane thiol and at the same time not observing sufficient gold atoms on the surface to support 1 : 1, 2 : 1 and 0 : 1 Au_{ad}/alkane thiol ratios. Additionally all the recent experimental and theoretical studies also strongly favour the 1 : 2 ratio models for dilute conditions[41] and 1 : 1 for high concentrations.[33,50] The optimisation of the models with 1 : 2 ratio provides two types of structures depending on the nature of the adsorbed species. The MeS^- and $MeS^•$ adsorbates form MeS–Au_{ad}–MeS type species with a strong interaction of the sulfur head group with the surface (see Fig. 2).

The MeSH species chemisorbed only to the Au_{ad} do not show any significant interactions with the gold atoms on the surface. Additionally, depending on the orientation of the methyl groups one can find two types of isomers where

the two methyl groups can be either in *cis* or in *trans* fashion.[42] For the MeS• species the *cis* structure is found to be the most favourable structure with the *trans* being only 1.0 kcal mol^{-1} higher in energy—thus an interchange between the two is a facile process as the computed kinetic barrier heights are small.[49] The computed binding energies resemble the trend found on the unreconstructed surface with the MeS• species being the most favourable with 39.9 and 30.0 kcal mol^{-1} margin for the MeS$^-$ and MeSH species, respectively. In this model structure, the MeS• species becomes clearly the most favourable with a very large margin with respect to the MeS$^-$ charged species, unlike in other model complexes.

The computed bond lengths for the species fall into two categories: (i) two short S–Au$_{ad}$ bonds in the range of 2.36 to 2.58 Å and (ii) two long Au$_{surf}$–S bonds in the range of 2.56–3.68 Å for all the three species. The S–Au$_{ad}$ bonds for all the three species are slightly longer than those found for Au–S bond lengths computed for the 1 : 1 ratio models but are essentially a complete Au–S bond (σ-type) with the Au$_{ad}$ and weak interactions to the surface (in the case of MeS$^-$ and MeS• species). The NBO analysis also suggests this bonding picture. The MeSH species has two predominant interactions: a strong σ-type 3p$_x$(S)–6s(Au) interaction and a weak 3s(S)–6s(Au) interaction to the Au$_{ad}$ atom with negligible contributions to the sulfur–gold atoms of the surface. The MeS$^-$ and MeS• species have a 3s(S)–6s(Au) interaction with the Au$_{ad}$ atoms and also the Au atom of the Au(111) surface. The σ-type 3p$_z$(S)–6s(Au) interaction is predominant in the Au–S bond of the sulfur–gold atoms of the surface while 3p$_x$(S)–6s(Au) is the strongest interaction in the Au$_{ad}$–S bond. However, the Au$_{ad}$–S bond has multiple contributions from the 3p$_x$(S)–6p$_x$(Au), 3p$_x$(S)–6d$_{xz}$(Au) and 3p$_x$(S)–6d$_{xy}$(Au) interactions. In order to evaluate the binding energies of a model possessing a structural motif of both 1 : 2 and 2 : 1 ratio of Au$_{ad}$/methyl thiol, we computed the binding energy of the 2 : 3 Au$_{ad}$/methyl thiol ratio model for the MeS• species (see Fig. 3). The binding energy for this model is only −40.0 kcal mol^{-1} and an additional vacancy on this model tends to increase the binding energy up to −23.3 kcal mol^{-1}. Additionally, we have also considered the two adatoms with two vacancies model proposed for a long chain alkyl thiol based on molecular dynamics calculations and GIXRD experiments.[41] This structure has a binding energy of only −28.2 kcal mol^{-1} (see Fig. 3).

As models with vacancies are energetically unfavourable compared to those of the others discussed previously (*vide infra*), we will focus our discussion only among the three models discussed above. Except for the 1 : 1 ratio of the Au$_{ad}$/methyl thiol model, the stability of the species follows the trend, MeSH < MeS– < MeS•. This is consistent with the fact that under neutral conditions, as is the case in the formation of SAMs, the S–H bond expected to cleave homolytically with an affordable kinetic barrier resulted in a radical species being adsorbed on the Au(111) surface.[100] Our calculations show a clear energetic preference for the presence of Au$_{ad}$ atoms on the Au(111) surface.

Among different Au$_{ad}$/methyl thiol ratio models, the 1 : 1 stabilises the MeS$^-$ species. Although this species is unlikely to occur in the neutral condition but only in a basic pH condition, the nature of the adsorbed species and thus the underlying structure can be pH dependent.[101] Both 2 : 1 and 1 : 2 Au$_{ad}$/methyl thiol models suggest MeS• being the most stable species with the former being more stable by 22.8 kcal mol^{-1}.

The 2 : 1 Au$_{ad}$/methyl thiol model with Au$_{ad}$–MeS•–Au$_{ad}$ species is however likely to form only in very high Au$_{ad}$ coverage and very low concentration of thiols. The usual experimental conditions however employ large excess of thiols to get SAMs and therefore a 1 : 2 Au$_{ad}$/methyl thiol model is most likely to result in the SAM formation as it had been proven in the recent experimental findings.[35,36,40,41,43] For this

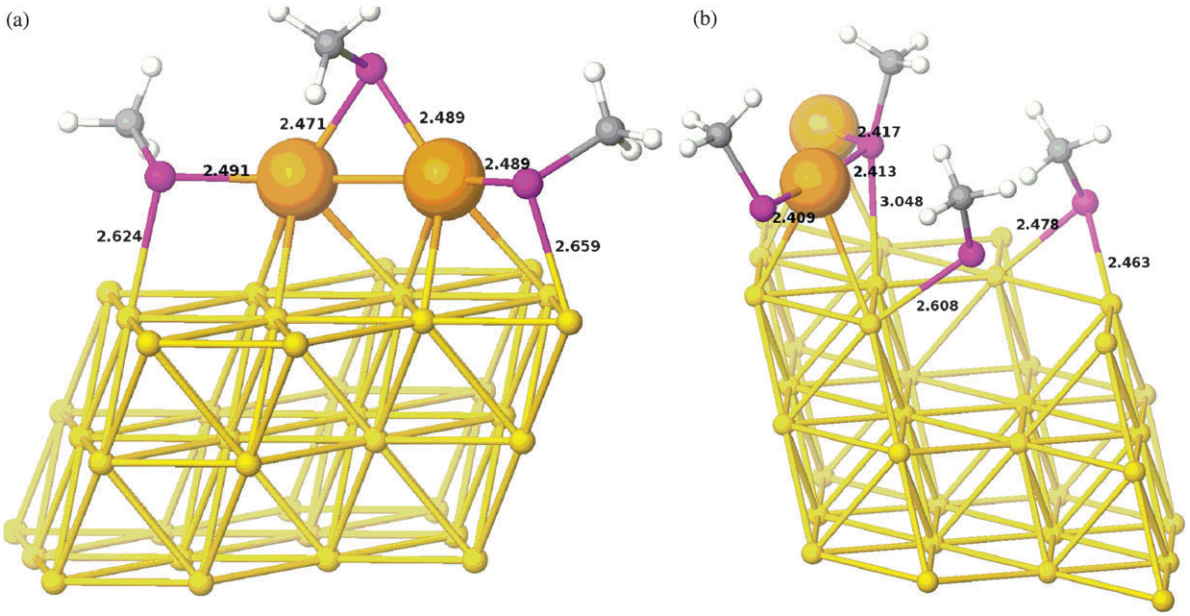

Fig. 3 The DFT structures of MeS• species for (a) the 2 : 3 Au$_{ad}$/methyl thiol model, (b) the SAM structure proposed by GIXRD and molecular dynamics simulations for long chain alkyl thiols.

ratio the MeS$^{\bullet}$–Au$_{ad}$–MeS$^{\bullet}$ is the most favourable species and this is consistent with the experimental as well as theoretical studies. Given the energetics of the different species, it is however very likely that different species having the formation energies within 2–3 kcal mol^{-1} are probably in equilibrium under real experimental conditions and therefore the actual SAM structures could be much more complex than what can be described by a single minimum energy structure.

Formation of ($\sqrt{3} \times \sqrt{3}$)R30° surface structure

As stated earlier the STM experiments and NIXSW, GIXRD experiments reveal a ($\sqrt{3} \times \sqrt{3}$)R30° surface structure for the adsorption of methyl thiol on the Au(111).[1–7] We have therefore considered the binding energy for this pattern and we have performed calculations only on two selected models with MeS$^{\bullet}$ being the adsorbate: the first one is on a clean Au(111) surface and the other is on a reconstructed surface. We have chosen the 1 : 1 ratio of the Au$_{ad}$/methyl thiol model for this purpose. The optimised structures of both models are shown in Fig. S3 (ESI†). On the clean surface the MeS$^{\bullet}$ species adopt a bridge structure like the one found for the isolated ones. However, due to the intermolecular interactions, the average Au–S bond lengths in the SAM structure are 2.54 and 2.67 Å which are about −0.05 and +0.07 Å shorter/longer than what is found in the isolated structures. The calculations provide a binding energy of −28.8 kcal mol^{-1} for this structure and this is 8.4 kcal mol^{-1} higher than in isolated systems. On the reconstructed surface with a 1 : 1 ratio of the Au$_{ad}$/methyl thiol model, the Au–S bond lengths do not deviate from those found for the isolated ones. In this model the SAM becomes more stable than the corresponding isolated structure by 1.1 kcal mol^{-1} (−43.7 kcal mol^{-1}) indicating the importance of intermolecular interactions for the stabilisation of regular array of SAM structures and the computed binding energy is consistent with the values reported in the literature.[36,38–40]

Adsorption of mono-/di-substituted alkyl and phenyl thiols on Au(111)

With the extensive data in hand for the methyl-thiol adsorption on Au(111), here we set out to understand the difference in the structure and energetics of the adsorption of higher alkyl-/phenyl-thiols on Au(111). Particularly we have focused on the energetics of dimethyl sulfide (MeSMe), diethyl sulfide (EtSEt), diphenyl sulfide (PhSPh) and methyl phenyl sulfide (MeSPh) in order to assess and understand the possible S–C cleavage on adsorption to Au(111). All the thiols mentioned above upon homolytic S–C cleavage form radical species which then chemisorb to the surface. The S–C bond cleavage on this reaction is expected to occur favourably, as the bond dissociation energy (BDE) of the S–C bond in all the thiols mentioned above is much lower than the BDE of the S–H bond in MeS–H species[102] (see Table S3, ESI†). The BDE is expected to be lowered on adsorption to the Au(111) as the S–X (X = H, C) bond weakens upon adsorption and such weakening of the bonds has been experimentally detected using the SERS spectroscopy for the dimethyl sulfide on gold.[103,104] This is also supported by the convincing spectroscopic evidence where the S–C cleavage has been observed for some alkyl thiols on the Ag surface.[105–107] The results gathered for the substituted thiols are summarised in Fig. S4 (ESI†). We have considered two scenarios for these species: the S–C bond undissociated species and a species formed by a homolytic S–C bond cleavage. As our previous results revealed, the radical species is the most stable one, we have computed the binding energies for both the unreconstructed and reconstructed surfaces for such species. In the reconstructed surface we have considered only the 1 : 1 and 1 : 2 Au$_{ad}$/thiol models as these models are more relevant to the experiments and also found to be energetically favourable in methyl thiol studies.

For the undissociated species, only the 1 : 1 Au$_{ad}$/thiols models are considered. The important structural parameters together with the binding energies are summarised in Table S4 (ESI†). In all the computed cases the reconstructed surface is more favourable than that of the clean surface. The undissociated species adopt quasi-atop configuration while the dissociated species adopt a bridge structure like the one

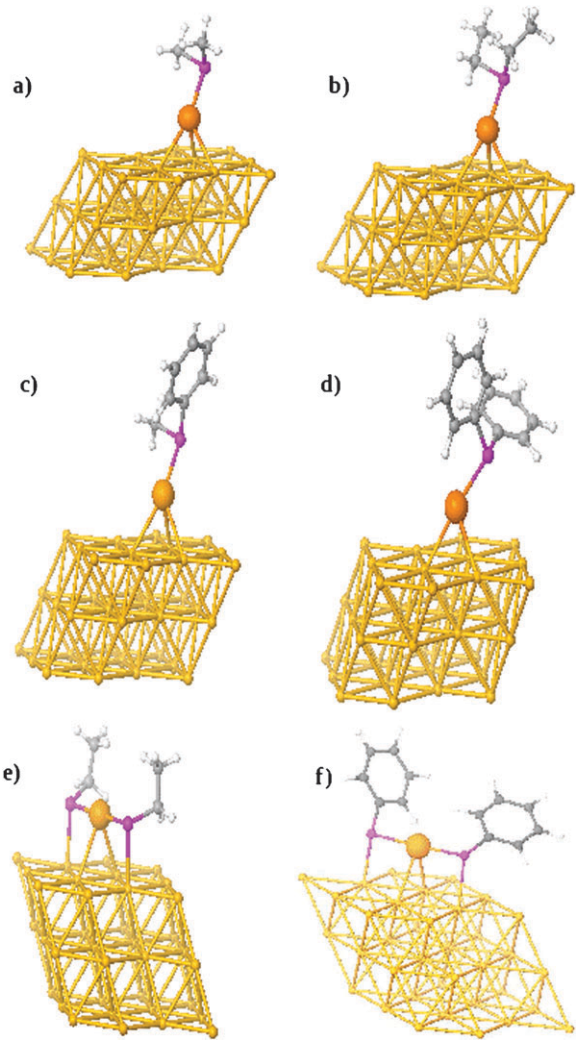

Fig. 4 The TPSS optimised structure of the 1 : 1 Au$_{ad}$/thiol model of (a) Me$_2$S, (b) Et$_2$S, (c) Ph$_2$S, (d) PhSMe and the 1 : 2 Au$_{ad}$/thiol model of (e) EtS$^{\bullet}$ and (f) PhS$^{\bullet}$. See Table S4 (ESI†) for important structural parameters.

that is observed for the simple alkyl thiols. The binding energy of Me_2S on the clean surface is only -3.3 kcal mol^{-1} and this is similar to the binding energies computed for the MeSH species adsorption. On a reconstructed 1 : 1 model the binding energy is -23.4 kcal mol^{-1} (also see Fig. 4). As expected, there is a significant gain in the stabilisation on the reconstructed surface, like in MeSH species there is a strong Au–S bond in the 1 : 1 model with a bond length of 2.43 Å. In the dissociated case, Me_2S will result in the formation of MeS$^{\bullet}$ and Me$^{\bullet}$ species whose binding energy is much lower due to strong gold–sulfur interaction. The general energetic trend for the Et_2S shifts to a lower binding energy with -13.0 kcal mol^{-1} on the clean surface and -24.6 kcal mol^{-1} on the reconstructed surface. Like in Me_2S, upon dissociation there is a large gain in the binding energies. For the EtS$^{\bullet}$ species the computed energetics and structure are similar to those computed for the MeS$^{\bullet}$ but the binding energies are shifted to slightly lower values (see Fig. S4, ESI†). For Ph_2S species as well, the 1 : 1 model is predicted to be more stable however the binding energy of Au_{ad}–Ph_2S is slightly higher (-19.7 kcal mol^{-1}) than the alkyl counterparts. The two phenyl groups on the sulfur atoms are in different positions, *i.e.* one lies about *ca.* perpendicular to the surface while the other lies *ca.* flat to the surface normal as reflected in the molecular tilt angles ζ (see Fig. 4 and Table S4, ESI†). The calculation predicts that the dissociated species are much more stable and different models computed for the dissociated species follow the same trend as the non-dissociated species (see Fig. S4, ESI†). Although the differences are small, there is a clear trend in the binding energies of the species, EtS$^{\bullet}$ > MeS$^{\bullet}$ > PhS$^{\bullet}$ > Et_2S > Me_2S > MeSH > PhSMe > Ph_2S. This trend is related to the electron donating ability of the substituent. In the 1 : 1 model there is a strong Au–S bond and significant stabilisation can be gained if an electron donating group is present on the sulfur. Among all the three cases studied, the 1 : 2 Au_{ad}/thiols model is found to be the most favourable. Moreover, the binding energy for PhS$^{\bullet}$ species on an unreconstructed surface is unexpectedly more stable than in a 1 : 1 reconstructed model in contrast to what was found for the alkyl species. In a high concentrated SAM, where the 1 : 2 model should be less favored for hindrance reasons, an unreconstructed surface is therefore expected.

4. Conclusions

The self-assembled monolayers offer a possible way to achieve spintronics devices—an emerging technological advancement exploiting the spin of electrons and their associated magnetic properties in solid-state devices and thus adding a new dimension to the existing devices.[108,109] The current trends in this area are the studies on simple aromatic compounds such as benzene and its substituted derivatives for spin transport properties.[108,109] Our finding of the radical nature of the thiols adsorbed in the Au(111) surface thus has direct implication as to see how this affects the transport properties.

Our comprehensive studies on methyl and substituted thiol molecules reveal many insights into the SAM structure. Our calculations suggest that the S–H bond cleaves homolytically leading to a radical centre which firmly adsorbs on the Au(111).

Our calculations are in general consistent with the reported experimental and theoretical results and thus reveal that the reconstructed Au(111) surface models are preferable over a clean unreconstructed Au(111) surface based on energetics arguments. In parallel with the experimental and theoretical evidences, our calculations indicate that a model with 1 : 2 Au_{ad}/thiols MeS$^{\bullet}$–Au_{ad}–MeS$^{\bullet}$ is energetically favourable compared to the clean and 1 : 1 ratio models. This suggests that the real structures in the SAMs are complex with a possible mixture of energetically similar configurations; such equilibrium can be perturbed by the experimental conditions (synthetic procedure, pH conditions, polarity of solvents employed, *etc*). The NBO analysis indicates that the Au_{ad}–S interactions are very strong and in 1 : 1 ratio models Au_{ad}–S bonds are partially covalent (~65% donation from sulfur). Similar results have been obtained with more complex substituted thiols. we have extended our studies in the subsequent section to substituted thiols particularly, dimethyl, diethyl, diphenyl and phenyl–methyl thiols to explore the energetic trends of these species compared to that of methyl thiols. The main focus was to address the S–C bond cleavage like the S–H cleavage in the methyl thiols. Our calculations indicate an energetically preferred homolytic S–C cleavage and thus a stronger RS$^{\bullet}$–Au(111) interaction. Studies on the reconstructed surface reveal that the 1 : 2 Au_{ad}/thiols ratio models are the one being the energetically favourable. The computed binding energies have the following trend: EtS$^{\bullet}$ > MeS$^{\bullet}$ > PhS$^{\bullet}$ > Et_2S > Me_2S > MeSH > PhSMe > Ph_2S and this is correlated to the electron donating ability of the groups attached to the sulfur atoms.

Notes and references

1 A. Ulman, *Chem. Rev.*, 1996, **96**, 1533; A. Ulman, *Acc. Chem. Res.*, 2001, **34**, 855.
2 G. E. Poirier, *Chem. Rev.*, 1997, **97**, 1117.
3 J.-C. Love, L. A. Estroff, J. K. Kriebel, R. G. Nuzzo and G. M. Whitesides, *Chem. Rev.*, 2005, **105**, 1103; A. Kumar, N. L. Abbott, H. A. Biebuyck, K. Enoc and G. M. Whitesides, *Acc. Chem. Res.*, 1995, **28**, 219.
4 G. Heimel, L. Romaner, E. Zojer and J.-L. Bredas, *Acc. Chem. Res.*, 2008, **41**, 721.
5 J. E. Houston and I. H. Kim, *Acc. Chem. Res.*, 2002, **35**, 547.
6 D. P. Woodruff, *Phys. Chem. Chem. Phys.*, 2008, **10**, 7211.
7 C. Vericat, M. E. Vela, G. A. Benitez, J. A. Martin Gago, X. Torrelles and R. C. Salvarezza, *J. Phys.: Condens. Matter*, 2006, **18**, 867.
8 A. Cornia, A. C. Fabretti, M. Pacchioni, L. Zobbi, D. Bonacchi, A. Caneschi, D. Gatteschi, R. Biagi, U. Del Pennino, V. De Renzi, L. Gurevich and H. S. Van der Zant, *Angew. Chem., Int. Ed.*, 2003, **42**, 1645.
9 M. Mannini, F. Pineider, P. Sainctavit, L. Joly, A. Fraile-Rodriguez, M.-A. Arrio, C. Cartier dit Moulin, W. Wernsdorfer, A. Cornia, D. Gatteschi and R. Sessoli, *Adv. Mater.*, 2009, **21**, 167.
10 M. Mannini, P. Sainctavit, R. Sessoli, C. Cartier dit Moulin, F. Pineider, M.-A. Arrio, A. Cornia and D. Gatteschi, *Chem.–Eur. J.*, 2008, **14**, 7530.
11 M. Fonin, S. Voss, M. Burgert, Yu. S. Dedkov, U. Groth and U. Ruediger, *J. Phys.*, 2008, **100**, 52070.
12 S. Voss, M. Burgert, M. Fonin, U. Groth and U. Ruediger, *Dalton Trans.*, 2008, 499.
13 S. Barraza-Lopez, M. C. Avery and K. Park, *Phys. Rev. B: Condens. Matter*, 2007, **76**, 224413.
14 E. Coronado, A. Forment-Aliaga, F. M. Romero, V. Corradini, R. Biagi, V. De Renzi, A. Gambardella and U. Del Pennino, *Inorg. Chem.*, 2005, **44**, 7693.

15 M. Mannini, F. Pineider, P. Sainctavit, C. Danieli, E. Otero, C. Sciancalepore, A. M. Talarico, M.-A. Arrio, A. Cornia, D. Gatteschi and R. Sessoli, *Nat. Mater.*, 2009, **8**, 194; M. Mannini, F. Pineider, C. Danieli, F. Totti, L. Sorace, Ph. Sanctavit, M.-A. Arrio, E. Otero, L. Joly, J. Criginski Cesar, A. Cornia and R. Sessoli, *Nature*, 2010, **468**, 417.
16 M. Mannini, L. Sorace, L. Gorini, F. M. Piras, A. Caneschi, A. Magnani, S. Menichetti and D. Gatteschi, *Langmuir*, 2007, **23**, 2389.
17 M. M. Matsushita, N. Ozaki, T. Sugawara, F. Nakamura and M. Hara, *Chem. Lett.*, 2002, 596.
18 G. Harada, H. Sakurai, M. M. Matsushita, A. Izuoka and T. Sugawara, *Chem. Lett.*, 2002, 1030.
19 M. Mannini, D. Rovai, L. Sorace, A. Perl, B. J. Ravoo, D. N. Reinhoudt and A. Caneschi, *Inorg. Chim. Acta*, 2008, **361**, 3525.
20 A. Bencini, G. Rajaraman, F. Totti and M. Tusa, *Superlattices Microstruct.*, 2009, **46**, 4; G. Rajaraman, A. Caneschi, D. Gatteschi and F. Totti, *J. Mater. Chem.*, 2010, **20**, 10747.
21 G. E. Poitier and E. D. Pylant, *Science*, 1996, **272**, 1145.
22 H. Sellers, A. Ulman, Y. Shnidman and J. E. Eilers, *J. Am. Chem. Soc.*, 1993, **115**, 9389.
23 H. Gronbeck, A. Curioni and W. Andreoni, *J. Am. Chem. Soc.*, 2000, **122**, 3839.
24 Y. Yourdshahyan, H. K. Zhang and A. M. Rappe, *Phys. Rev. B: Condens. Matter*, 2001, **63**, 081405.
25 M. Tachibana, K. Yoshizawa, A. Ogawa, H. Fujimoto and R. Hofmann, *J. Phys. Chem. B*, 2002, **106**, 12727.
26 T. Hayashi, Y. Morikawa and H. Nozoye, *J. Chem. Phys.*, 2001, **114**, 7615.
27 C. Vargas, P. Giannozzi, A. Selloni and G. Scoles, *J. Phys. Chem. B*, 2001, **105**, 9509.
28 J. Gottschalck and B. Hammer, *J. Chem. Phys.*, 2002, **116**, 784.
29 M. L. Molina and B. Hammer, *Chem. Phys. Lett.*, 2002, **360**, 264.
30 Y. Morikawa, C. C. Liew and H. Nozoye, *Surf. Sci.*, 2002, **514**, 389.
31 M. G. Roper, M. P. Skegg, C. J. Fisher, J. J. Lee, V. R. Dhank, D. P. Woodruff and R. G. Jones, *Chem. Phys. Lett.*, 2004, **389**, 87.
32 H. Kondoh, M. Iwasaki, T. Shimada, K. Amemiya, T. Yokoyama, T. Ohta, M. Shimomura and S. Kono, *Phys. Rev. Lett.*, 2003, **90**, 066102.
33 M. Yu, N. Bovet, C. J. Satterley, S. Bengió, K. R. J. Lovelock, P. K. Milligan, R. G. Jones, D. P. Woodruff and V. Dhanak, *Phys. Rev. Lett.*, 2006, **97**, 166102; A. Chaudhuri, D. C. Jackson, T. J. Lerotholi, R. G. Jones, T.-L. Lee, B. Detlefs and D. P. Woodruff, *Phys. Chem. Chem. Phys.*, 2010, **12**, 3229.
34 P. Maksymovych, D. C. Sorescu, D. Dougherty and T. Y. Yates, Jr., *J. Phys. Chem. B*, 2005, **109**, 22463.
35 P. Maksymovych, D. C. Sorescu and J. T. Yates, Jr., *Phys. Rev. Lett.*, 2006, **97**, 146103.
36 H. Grönbeck and H. Häkkinen, *J. Phys. Chem. B*, 2007, **111**, 3325.
37 R. Mazzarello, A. Cossaro, A. Verdini, R. Rousseau, L. Casalis, M. F. Danisman, L. Floreano, S. Scandolo, A. Morgante and G. Scoles, *Phys. Rev. Lett.*, 2007, **98**, 016102.
38 A. Nogoya and Y. Morikawa, *J. Chem. Phys.*, 2007, **19**, 365245.
39 J.-G. Wang and A. Selloni, *J. Phys. Chem. C*, 2007, **111**, 12149.
40 A. Cossaro, R. Mazzarello, R. Rousseau, L. Casalis, A. Verdini, A. Kohlmeyer, L. Floreano, S. Scandolo, A. Morgante, M. L. Klein and G. Scoles, *Science*, 2008, **321**, 943.
41 P. Maksymovych and J. T. Yates, *J. Am. Chem. Soc.*, 2008, **130**, 7518.
42 P. Carro, R. Salvarezza, D. Torres and F. Illas, *J. Phys. Chem. C*, 2008, **112**, 19121.
43 N. A. Kautz and S. A. Kandel, *J. Am. Chem. Soc.*, 2008, **130**, 6908; F.-S. Li, W. Zhou and Q. Guo, *Phys. Rev. B: Condens. Matter*, 2009, **79**, 113412.
44 O. Voznyy and J. J. Dubowski, *Langmuir*, 2009, **25**, 7353.
45 H. Groenbeck, H. Haekkinen and R. L. Whetten, *J. Phys. Chem. C*, 2008, **112**, 15940.
46 D. Jiang, *Chem. Phys. Lett.*, 2009, **477**, 90.
47 A. Franke and E. Pehlke, *Phys. Rev. B: Condens. Matter*, 2009, **79**, 235441.
48 D. Jiang and S. Dai, *J. Phys. Chem. C*, 2009, **113**, 3763.
49 J. Wang and A. Selloni, *J. Phys. Chem. C*, 2009, **113**, 3763.
50 A. Chaudhuri, T. J. Lerotholi, D. C. Jackson, D. P. Woodruff and R. G. Jones, *Phys. Rev. B: Condens. Matter*, 2009, **79**, 195439; A. Chaudhuri, T. J. Lerotholi, D. C. Jackson, D. P. Woodruff and V. Dhanak, *Phys. Rev. Lett.*, 2009, **102**, 126101.
51 E. Torres, A. T. Blumenau and P. U. Biedermann, *Phys. Rev. B: Condens. Matter*, 2009, **79**, 075440.
52 O. Voznyy, J. J. Dubowski, J. T. Yates and P. Maksymovych, *J. Am. Chem. Soc.*, 2009, **113**, 12989.
53 C. J. Mundy, F. Mohamed, F. Schiffman, G. Tabacchi, H. Forbert, W. Kuo, J. Hutter, M. Krack, M. Iannuzzi, M. McGrath, M. Guidon, T. D. Kuehne, T. Laino, J. VandeVondele and V. Weber, *CP2K software package*, http://cp2k.berlios.de.
54 J. VandeVondele, M. Krack, F. Mohamed, M. Parrinello, T. Chassaing and J. Hutter, *Comput. Phys. Commun.*, 2005, **167**, 103.
55 G. Lippert, J. Hutter and M. Parrinello, *Mol. Phys.*, 1997, **92**, 477.
56 G. Lippert, J. Hutter and M. Parrinello, *Theor. Chem. Acc.*, 1999, **103**, 124.
57 A. D. Becke, *Phys. Rev. A*, 1988, **38**, 3098.
58 C. Lee, W. Yang and R. G. Parr, *Phys. Rev. B: Condens. Matter*, 1988, **37**, 785.
59 J. Tao, J. P. Perdew, V. N. Staroverov and G. E. Scuseria, *Phys. Rev. Lett.*, 2003, **91**, 146401; A. Ruzsinszky, J. P. Perdew and G. I. Csonka, *J. Phys.Chem. A*, 2005, **109**, 11015.
60 A. Vargas, G. Santarossa, M. Lannuzzi and A. Baiker, *J. Phys. Chem. C*, 2008, **112**, 10200.
61 G. Santarossa, A. Vargas, M. Iannuzzi, C. A. Pignedoli, D. Passerone and A. Baiker, *J. Chem. Phys.*, 2008, **129**, 234703.
62 A. Ferral, E. M. Patrito and P. Paredes-Olivera, *J. Phys. Chem. B*, 2006, **110**, 17050; Y. Yourdshahyan, H. K. Zhang and A. M. Rappe, *Phys. Rev. B: Condens. Matter*, 2001, **63**, 81405.
63 *Jaguar 7.0*, Schrödinger, Portland, OR 97204.
64 A. D. Becke, *J. Chem. Phys.*, 1993, **98**, 5648; P. J. Stephens, F. J. Devlin, C. F. Chabalowski and M. J. Frisch, *J. Phys. Chem.*, 1994, **98**, 11623.
65 P. J. Hay and W. R. Wadt, *J. Chem. Phys.*, 1985, **82**, 270; P. J. Hay and W. R. Wadt, *J. Chem. Phys.*, 1985, **82**, 284; P. J. Hay and W. R. Wadt, *J. Chem. Phys.*, 1985, **82**, 299.
66 P. C. Hariharan and J. A. Pople, *Theor. Chim. Acta*, 1973, **28**, 213; M. M. Francl, W. J. Petro, W. J. Hehre, J. S. Binkley, M. S. Gordon, D. J. DeFrees and J. A. Pople, *J. Chem. Phys.*, 1982, **77**, 3654; V. Rassolov, J. A. Pople, M. Ratner and T. L. Windus, *J. Chem. Phys.*, 1998, **109**, 1223.
67 J.-G. Zhou and F. Hagelberg, *Phys. Rev. Lett.*, 2006, **97**, 045505.
68 L. Dubois, B. Zegarski and R. Nuzzo, *J. Chem. Phys.*, 1993, **98**, 678; C. Kodama, T. Hayashi and H. Nozoye, *Appl. Surf. Sci.*, 2001, **169**, 264; G. Liu, J. Rodriguez, J. Dvorak, J. Hrbek and T. Jirsak, *Surf. Sci.*, 2002, **122**, 3839.
69 I. Rzeznicka, J. Lee, P. Maksymovych and J. Yates, Jr., *J. Phys. Chem. B*, 2005, **109**, 15992.
70 H. Gronbeck, A. Curioni and W. Andreoni, *J. Am. Chem. Soc.*, 2000, **122**, 3839.
71 Y. Akinaga, T. Nakajima and K. Hirao, *J. Chem. Phys.*, 2001, **114**, 8555.
72 J. Gottschalck and B. Hammer, *J. Chem. Phys.*, 2002, **116**, 76.
73 R. G. Nuzzo, B. R. Zegarski and L. H. Dubois, *J. Am. Chem. Soc.*, 1987, **109**, 733.
74 M. G. Roper, M. P. Skegg, C. J. Fisher, J. J. Lee, V. R. Dhanak, D. P. Woodruff and R. G. Jones, *Chem. Phys. Lett.*, 2004, **389**, 8791.
75 S. Franzen, *Chem. Phys. Lett.*, 2003, **381**, 315.
76 F. P. Cometto, P. Paredes-Olivera, V. A. Macagno and E. M. Patrito, *J. Phys. Chem. B*, 2005, **109**, 21737.
77 G. Liu, J. A. Rodriguez, J. Dvorak, J. Hrbek and T. Jirsak, *Surf. Sci.*, 2002, **505**, 295.
78 P. C. Rusu and G. Brocks, *J. Phys. Chem. B*, 2006, **110**, 22628.
79 Y. Yourdshahyan and A. M. Rappe, *J. Chem. Phys.*, 2002, **117**, 825.
80 S. Higai, J. Nara and T. Ohno, *J. Chem. Phys.*, 2004, **121**, 970.
81 S. S. Jang, Y. H. Jang, Y.-H. Kim, W. A. Goddard III, A. H. Flood, B. W. Laursen, H.-R. Tseng, J. F. Stoddart, J. O. Jeppesen, J. W. Choi, D. W. Steuerman, E. Deionno and J. R. Heath, *J. Am. Chem. Soc.*, 2005, **127**, 1563.

82 J. Nara, S. Higai, Y. Morikawa and T. Ohno, *J. Chem. Phys.*, 2004, **120**, 6705.
83 A. Johansson and S. Stafstrom, *Chem. Phys. Lett.*, 2000, **322**, 301.
84 R. Liu, S.-H. Ke, H. U. Baranger and W. J. Yang, *J. Chem. Phys.*, 2005, **122**, 44703.
85 E. Goll, M. Ernst, F. Moegle-Hofacker and H. Stoll, *J. Chem. Phys.*, 2009, **130**, 234112.
86 A. Krishtal, K. Vanommeslaeghe, A. Olasz, T. Veszpremi, C. Van Alsenoy and P. Geerlings, *J. Chem. Phys.*, 2009, **130**, 174101.
87 Md. E. Ali, P. M. Oppeneer and S. N. Datta, *J. Phys. Chem. B*, 2009, **113**, 5545.
88 L. Lao, H. Ke, G. Fu, X. Xu and Y. Yan, *J. Chem. Theory Comput.*, 2009, **5**, 86.
89 K. Pluhackova, S. Grimme and P. Hobza, *J. Phys. Chem. A*, 2008, **112**, 12469.
90 M. P. Johansson, A. Lechtken, D. Schooss, M. M. Kappes and F. Furche, *Phys. Rev. A*, 2008, **77**, 053202.
91 W. Andreoni, A. Curioni and H. Gronbeck, *Int. J. Quantum. Chem.*, 2000, **80**, 598; M. Hasan, D. Bethell and M. Brust, *J. Am. Chem. Soc.*, 2002, **124**, 1132.
92 E. Garand and P. A. Rowntree, *J. Phys. Chem. B*, 2005, **109**, 12927; P. Rowntree, P.-C. Dugal, D. Hunting and L. Sanche, *J. Phys. Chem.*, 1996, **100**, 4546.
93 L. Kankate, A. Turchanin and A. Goelzhauser, *Langmuir*, 2009, **25**, 10435.
94 M. Tachibana, K. Yoshizawa, A. Ogawa, H. Fujimoto and R. Hoffmann, *J. Phys. Chem. B*, 2002, **106**, 12727.
95 A. Calzolari and R. D. Felice, *J. Phys.: Condens. Matter*, 2007, **19**, 305018.
96 B. Kong, Y. Kim and S. I. Choi, *Bull. Korean Chem. Soc.*, 2008, **29**, 1843.
97 C. Liu, J. Hu and G. Lu, *Wuhan Univ. J. Nat. Sci.*, 2007, **12**, 522.
98 F.-M. Boldt, N. Baltes, K. Borgwarth and J. Heinze, *Surf. Sci.*, 2005, **597**, 51.
99 A. Sladek, K. Angermaier and H. Schimbauer, *Chem. Commun.*, 1996, 1959; A. Sladek, H. Schimbauer and B. Natuforsch, *Chem. Sci.*, 1996, 1207; M. W. Heaven, A. Dass, P. S. White, K. M. Holt and R. W. Murray, *J. Am. Chem. Soc.*, 2008, **130**, 3754.
100 Our preliminary calculations of barrier heights indicates that at the transition state the species possesses significant radical character, indicating again the preference for the homolytic cleavage, G. Rajaraman and F. Totti, in preparation.
101 It is also important to note that in a highly basic medium desorption of the alkane thiols will also be significant[96].
102 S. Benson, *Chem. Rev.*, 1978, **78**, 23.
103 J. K. Lim, I.-H. Kim, K.-H. Kim, K. S. Shin, W. Kang, J. Choo and S.-W. Joo, *Chem. Phys.*, 2006, **330**, 245.
104 S. W. Joo, S. W. Han and K. Kim, *Appl. Spectrosc.*, 2000, **54**, 378.
105 Y. Hyeon, Y. Kwan and M. S. Kim, *J. Phys. Chem.*, 1990, **94**, 2552.
106 C. J. Sandroff and D. R. Herschbach, *J. Phys. Chem.*, 1982, **86**, 3277.
107 K. L. Kim, S. J. Lee and K. Kim, *J. Phys. Chem. B*, 2004, **108**, 9216.
108 N. Baadji, M. Piacenza, T. Tugsuz, S. F. Della, G. Maruccio and S. Sanvito, *Nat. Mater.*, 2009, **8**, 813; G. Zulczewski, S. Sanvito and M. Coey, *Nat. Mater.*, 2009, **8**, 693; R. Zhang, G. Ma, R. Li, Z. Qian, Z. Shen, X. Zhao, S. Hou and S. Sanvito, *J. Phys.: Condens. Matter*, 2009, **21**, 335301.
109 A. Giusti, G. Charron, S. Mazerat, J.-D. Compain, P. Mialane, A. Dolbecq, E. Riviere, W. Wernsdorfer, B. Ngo, B. Keita, L. Nadjo, A. Filoramo, J.-P. Bourgoin and T. Mallah, *Angew. Chem., Int. Ed.*, 2009, **48**, 4949; W. Wernsdorfer, *Nat. Nanotechnol.*, 2009, **4**, 145; L. Bogani and W. Wernsdorfer, *Nat. Mater.*, 2008, **7**, 179.